RSC Publishing Faraday Discussions

Templated growth of gold satellites on dimpled silica cores

Journal:	*Faraday Discussions*
Manuscript ID	FD-ART-02-2016-000022.R1
Article Type:	Paper
Date Submitted by the Author:	26-Feb-2016

Complete List of Authors:	Chomette, Cyril; ICMCB, Duguet, Etienne; Univ. Bordeaux, ICMCB/CNRS Mornet, Stéphane; CNRS, Institute of solid state chemistry and condensed matter Yammine, Elham; Institut de Chimie de la Matiere Condensee de Bordeaux Manoharan, Vinothan; Harvard University, Department of Physics; Harvard University, School of Engineering and Applied Sciences Schade, Nicholas; Harvard University, Department of Physics Hubert, Céline; CRPP, Ravaine, Serge; Centre de Recherche Paul Pascal (UPR 8641, CNRS), Perro, Adeline; Institut des Sciences Moleculaires Treguer, Mona; ICMCB-CNRS, Chemistry

Faraday Discussion

ARTICLE

Templated growth of gold satellites on dimpled silica cores

C. Chomette,[a] E. Duguet,[a]* S. Mornet,[a] E. Yammine,[a] V. N. Manoharan,[b,c] N. B. Schade,[c] C. Hubert,[d] S. Ravaine,[d]* A. Perro[e] and M. Tréguer-Delapierre[a]*

Received 00th January 20xx,
Accepted 00th January 20xx

DOI: 10.1039/x0xx00000x

www.rsc.org/

We synthesize robust clusters of gold satellites positioned with tetrahedral symmetry on the surface of a patchy silica core by adsorption and growth of gold on the patches. First we conduct emulsion polymerization of styrene in the presence of 52 nm silica seeds whose surface has been modified with methacryloxymethyltriethoxysilane (MMS). We derive four-dimple particles from the resulting silica/polystyrene tetrapods. Polystyrene chains are covalently bound to the silica surface within the dimples due to the MMS grafts and they may be thiolated to induce adsorption of 12 nm gold particles. Using chloroauric acid, ascorbic acid and sodium citrate at room temperature, we grow gold from these 12 nm seeds without detachment from or deformation of the dimpled silica surface. We obtain gold satellites of tunable diameter up to 140 nm.

1 Introduction

Colloidal particles with anisotropic shape or chemical functionality are building blocks for directed assembly of new materials.[1–4] For instance, particles with chemical anisotropy can assemble into unusual lattices[5] and dimpled particles can bind to spherical particles in a lock-and-key scheme due to depletion forces.[6] Both types of anisotropic particles can be used to assemble clusters of controlled size as well.[6,7]

Gold patches are of special interest because of their intrinsic optical properties and the ease with which their surfaces can be chemically modified. One way to prepare particles with gold patches is through physical vapor deposition of gold onto a monolayer or multilayer of spherical particles,[5,8,9] but this technique suffers from limited versatility and scalability.[5] An alternative method is to seed the growth of gold patches using small silver patches in a surface-conformal strategy.[10] Such a strategy would be quite easily up-scaled, but the size, number, and position of the gold patches then remain uncontrolled, because of the random positioning of the silver precursor patches.[11] One may instead nucleate and grow gold on isotropic particles, but this yields homogeneous gold coatings[12,13] or gold patches of uncontrolled size and position.[14] Therefore synthesis routes that permit control over gold patches in colloidal batch quantities have remained elusive.

One simple route would be to start with particles with highly controlled, symmetric patches, and then to modify them with gold. However, there are only a few established protocols for the synthesis of particles with controlled numbers and arrangements of patches or dimples of any sort, *e.g.* with linear, triangular or tetrahedral symmetry. Based on the steric hindrance phenomenon, they generally involve the confinement of a controlled number of spherical particles (which become the patches, patch precursors or dimple precursors) in a droplet, through sticky protrusions or at the surface of another colloid. For instance, Kim *et al*. stabilized oil-in-water emulsions with negatively-charged polystyrene (PS) particles and then photopolymerized the oil to obtain patchy microparticles.[15] Conversely, Kraft *et al*. prepared polymeric particles bearing liquid protrusions and then polymerized the liquid.[16] Wang and colleagues exploited the direct confinement by droplets of particles with specific surface functionalities.[7,17]

We recently reported the synthesis of silica particles with dimples arranged symmetrically, such that the number (1, 2, 3, 4, 6 or 12) and depth of dimples may be tuned.[18,19] Anchored PS chains reside at the bottom of each dimple and may be chemically modified to be sticky in specific assembly conditions.

In the present paper, we describe the use of these dimpled silica particles to adsorb and grow gold nanoparticles as metallic patches. Each dimple ultimately serves as a cradle for a single gold particle, and thus the dimple arrangement determines the final number, size, and positions of the gold satellites. We first explain some new insights regarding features of the residual PS chains in the dimples, and then we describe how we chemically modify them with thiol groups such that they interact favorably with gold nanoparticles. We next report the adsorption of citrate-stabilized gold

[a] CNRS, Univ. Bordeaux, ICMCB, UPR 9048, F-33600 Pessac, France.
[b] Harvard Univ., School of Engineering and Applied Sciences, Cambridge, MA 02138, USA.
[c] Harvard Univ., Department of Physics, Cambridge, MA 02138, USA.
[d] CNRS, Univ. Bordeaux, CRPP, UPR 8641, F-33600 Pessac, France.
[e] Univ. Bordeaux, CNRS, ISM, UMR 5255, F-33405 Talence, France.

Electronic Supplementary Information (ESI) available: TEM images of silica/polystyrene tetrapods from silica seeds previously surface-modified with acetoxypropyltrimethoxysilane; Pictures of the nitrobenzyl pyridine assay on dimpled silica particles before and after the chloromethylation reaction. See DOI: 10.1039/x0xx00000x

nanoparticles within the dimples and their subsequent growth according to three different synthesis recipes that we investigated. Here we focus on particles with four dimples, but the same strategy could be used with any other number of dimples.

2 Materials and methods

2.1 Materials

We used styrene (Sigma-Aldrich, 99%), methacryloxymethyl-triethoxysilane (MMS, ABCR, 98%), acetoxypropyltrimethoxy-silane (AMS, ABCR), sodium persulfate (Sigma-Aldrich, 99%), Symperonic® NP30 (Aldrich), sodium dodecylsulfate (SDS, Sigma-Aldrich, > 90%), tetraethoxysilane (TEOS, Sigma-Aldrich, 99%), ammonia (28–30% in water, SDS), $KAuCl_4$ (Sigma-Aldrich, 98%), $HAuCl_4.3H_20$ (Sigma-Aldrich, 99.9%), trisodium citrate (Sigma-Aldrich, 99%), $SnCl_4$ (Sigma-Aldrich, >99%), hydrochloric acid (37%, Sigma-Aldrich) and ammonia (28–30% in water, SDS), NaSH (Alfa-Aesar, 98%), $NaBH_4$ (Sigma-Aldrich, 96%), cetyltrimethylammonium bromide (CTAB, Sigma-Aldrich, 99%), and ascorbic acid (Sigma-Aldrich, 99%) as we received them. We obtained deionized water with a resistivity of 18.2 Ω·cm at 25°C from a Milli-Q system (Millipore). We purchased tetrahydrofuran (THF), dimethylformamide (DMF), chloroform, and absolute ethanol from Sigma-Aldrich. Lastly, we prepared butyl chloromethyl ether according to a recipe already published.[20]

2.2 Synthesis of dimpled silica particles

We prepared batches of tetrapods, consisting of a central silica core and four PS satellite nodules each, by seeded-growth emulsion polymerization of styrene, according to a procedure we published previously.[21-23] For a typical batch, we used 52 nm silica particles whose surface had been modified with MMS (0.5 molecule.nm^{-2}) as seeds (18×10^{15} particles/L) for the aqueous emulsion polymerization of styrene (100 g/L) at 70°C for 6 h in the presence of sodium persulfate (0.5 g/L) and a surfactant mixture (3 g/L) of Symperonic® NP30 and SDS (5 wt.%). The monomer-to-polymer conversion efficiency was 78%. Transmission electron microscopy revealed that the resulting batch consisted of tetrapods (73%), tripods (16%), hexapods (6%), mono-bipods (4%) and pentapods (1%).

We regrew the silica cores to create dimples using a method that we had also reported previously.[18,19] We prepared a mixture of 450 mL ethanol and 35 mL ammonia (1 M) and added first 10 mL of the polymerization medium containing 3.6×10^{14} tetrapods and then 4.8 mL of TEOS at a rate of 1 mL/h. We dissolved the PS satellite nodules by performing three centrifugation/redispersion cycles in THF, which leaves the dimples in place. The final batch contains 110 nm silica particles bearing four (74%), three (18%), six (5%), one/two (2%) or five (1%) dimples. In parallel experiments, we performed the synthesis using AMS instead of MMS for the preliminary surface modification of the silica seeds.

2.3 Characterization of the residual PS macromolecules at the bottom of the dimples

We collected, dried, and weighed the first THF supernatant containing the dissolved PS chains, and then dissolved it again in THF at a mass concentration of 1 mg/mL for size exclusion chromatography (SEC) experiments (UV detector at 260 nm and 0.2 vol.% of trichlorobenzene as standard).

2.4 Synthesis of citrate-stabilized gold nanoparticles

Our recipe was inspired by a previously reported technique.[24] In a 1-L round bottom flask maintained at a temperature of 100°C, we sequentially added 700 mL water, 314 mg $KAuCl_4$ diluted in 50 mL water, and 1.53 g trisodium citrate diluted in 75 mL water. The solution changed from yellow to colourless, bluish gray, and then red. We let the dispersion react for 15-20 min at 100°C. TEM images showed that the average diameter of the gold nanoparticles is 12 nm.

2.5 Thiolation of the residual PS macromolecules at the bottom of the dimples

We have already reported on the chloromethylation stage of the dimples' surface elsewhere.[19] Briefly, after transferring the as-prepared dimpled silica particles in chloroform, we added butyl chloromethyl ether in chloroform (3 M; 5 mL) and 0.3 mL $SnCl_4$. We set the temperature to 45°C and then aged the mixture overnight. Finally we washed the dispersion with three cycles of centrifugation/redispersion in HCl solution (4 wt.% in water) and then in water/ethanol (50/50 wt.%) before redispersing in 20 mL of DMF. We performed the thiolation stage after redispersion of 10^{13} chloromethylated patchy particles in ethanol. We added 2 g NaSH in 10 mL of ethanol and let the system react overnight under stirring. Finally, we washed the particles 5 times by centrifugation at 10,000 g for 15 min in ultrapure ethanol. At this time, the sample could be stored in ethanol. Before use, we transferred the particles into water, and then reduced the potential disulfide bonds by adding a few drops of an aqueous solution of 1 M $NaBH_4$. Finally we washed the dispersion by centrifugation and stored it in degassed water. To confirm the presence of thiol groups, we incubated the particles with the citrate-stabilized gold nanoparticles in water in a gold-to-silica particle ratio of 400:1. After overnight incubation over stirring, we removed the excess gold nanoparticles by centrifugation using ultrapure water at 5,000 g for 10 min and then we adjusted the concentration of the patchy silica particles to 9 x 10^{11} particles/mL.

2.6 Seeded-growth of gold nanoparticles within the dimples

We performed experiments with the goal of enlarging the diameter of the gold seeds, assuming that there is one gold seed per dimple. We investigate three different well-known seeded-growth recipes in solution.

Recipe #1: We took 20 mL of the thiolated patchy particle dispersion seeded with citrate-stabilized gold nanoparticles, and added it to 250 mL of an aqueous solution containing

CTAB (0.015 M), ascorbic acid (1 mM) and $HAuCl_4$ (0.5 mM) at 35°C for one hour. The resulting solution contained a small amount of free gold nanoparticles, which we could remove by centrifugation.

Recipe #2: We took 15 mL of the thiolated patchy particle dispersion seeded with citrate-stabilized gold nanoparticles, centrifuged it, dispersed it in 15 mL sodium citrate solution (2.2 mM), and transferred it into a 20 mL flask. We heated the dispersion to 90°C and then added 0.2 mL of $HAuCl_4$ (25 mM) in two equal fractions at 30-minute intervals. We assumed the gold nanoparticle concentration was roughly 3×10^{12} particles/mL. After 30 min, we removed 5.5 mL of the reacting volume from the flask and added 5.3 mL ultrapure water with 0.2 mL citrate sodium solution (60 mM). After temperature stabilization (5 min), we considered the growth cycle of the process completed. Finally, to stop the process, we allowed the solution to cool down to room temperature after completion of the last cycle. By repeating this process, we grew the gold particles within each dimple through up to 9 iterations.

Recipe #3: We took 1 mL of the thiolated patchy particle dispersion seeded with citrate-stabilized gold nanoparticles, and placed it in a three-neck 20-mL round bottom flask. The volume of the suspension contained between 10^{10} and 10^{12} gold seeds. To this we added a 10-mL aliquot of precursor solution A, containing $HAuCl_4$, $3H_20$, and 10 ml of reducing solution A', containing trisodium citrate and ascorbic acid. We added these solutions separately at room temperature through syringes via a peristaltic pump under vigorous stirring over a period of about 45 min (13.3 mL/h). Immediately after this was complete, we brought the mixture to boiling and maintained this temperature for about 30 min. Finally, we allowed the solution to cool down.

We prepared solution A by diluting a $HAuCl_4$, $3H_2O$ stock solution (0.2% w/v) to 10 mL. Similarly, we prepared solution A' by diluting a mixture of an ascorbic acid solution (1% w/v) and a trisodium- citrate solution (1% w/v) to 10 mL as well. The relative volume ratios of all three stock solutions was always 8:4:1. We estimated the volume of the gold precursor solution $V_{Au\ solution}$ required to grow the seeds from an initial diameter $D_{initial}$ to a final diameter D_{final} by using the following equation:

$$V_{Au\ solution} = \rho_{Au} N_{Au} \pi (D_{final}^3 - D_{initial}^3)/6 C_{Au\ solution} M_{Au}$$

where ρ_{Au} is the density of gold, M_{Au} the gold molar mass, and N_{Au} the number of gold nanoparticles in the considered volume.

We diluted the solution to obtain a final volume of 10 mL before loading it into the syringe and initiating the growth process.

3 Results and discussion

Our multistep synthesis route to dimpled silica particles is summarized in Scheme 1 and was reported previously.[18,19,21-23] Transmission electron microscopy (TEM) revealed that our silica/PS tetrapod mixture contained 73% tetrapods with byproducts ranging from monopods to hexapods. After regrowing the silica and dissolving the polystyrene to develop dimples on the particles, 74% of the contents were 110-nm silica particles bearing four dimples with a depth of about 27 nm. The byproducts are dimpled silica particles derived from the other multipods in the same proportions.

We previously showed that PS bumps remain at the bottom of the dimples (Fig. 1a,b), and we postulated that these grafted PS macromolecules result from the copolymerization of styrene with MMS.[18,19] To test this hypothesis, we performed the same synthesis of PS/silica tetrapods and then dimpled particles, but we replaced MMS with acetoxypropyltrimethoxysilane (AMS). The acetoxy end of AMS is saturated and therefore cannot polymerize according to a chain-growth mechanism. The resulting tetrapods were not as well-defined (see ESI Fig. §1) and, as we have already reported,[25] we found that they fall down onto TEM grids more frequently. Nevertheless, in the TEM image of a dimpled silica particle derived from one of these tetrapods, the PS bumps did not appear within the dimples (Fig. 1c). This confirms the origin of the grafted PS macromolecules and the role of MMS at their anchoring points.

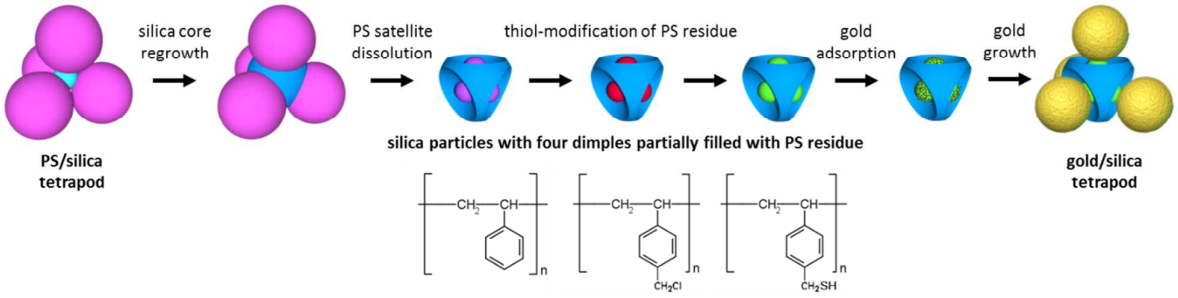

Scheme 1: Main steps of the synthesis of gold/silica tetrapods from PS/silica tetrapods via seeded growth of gold within the dimples.

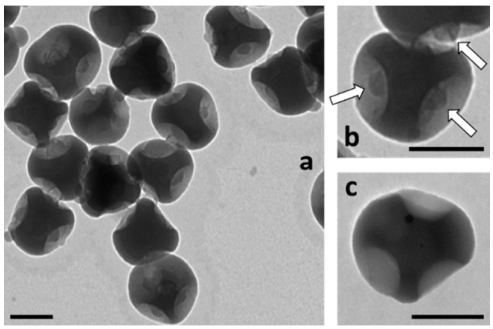

Figure 1: Transmission electron micrographs of silica particles with four dimples each, obtained from MMS-modified silica seeds (a and b) and from AMS-modified silica seeds (c). White arrows identify polystyrene bumps at the bottom of the dimples. Scale bars are 100 nm.

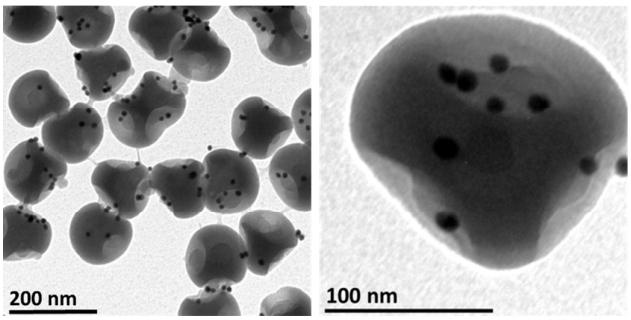

Figure 2: Transmission electron micrographs of the dimpled silica particles after thiol-modification of the PS chains at the bottom of the dimples and incubation with citrate-stabilized gold nanoparticles.

The length of the grafted macromolecules had been studied on alumina or silica/PS or poly(ethyl)acrylate core-shell particles obtained in similar emulsion polymerization conditions, using silanes as surface coupling agents.[26-28] The average molar mass and molar mass distribution of the grafted chains were often reported higher than those of the free macromolecules. In some cases, the authors pointed to siloxane bonding between the grafted molecules, suggesting that the MMS grafts serve as cross-linking groups. They assumed that the average molar masses of the grafted and non-grafted chains would be the same otherwise. Using our SEC experiments performed on the non-grafted PS chains recovered at the stage of their dissolution in THF, we found an average molar mass of 540,000 g/mol (number-averaged) or 980,000 g/mol (weight-averaged). These values are comparable to those typically obtained from emulsion polymerization. It means that these chains are long and can readily serve as extended anchoring arms for interacting with gold satellites.

However, since our goal was to develop covalent coupling with gold satellites, we could not use the PS bumps in their original state. Instead, we modified the PS macromolecules with thiol groups, which are well-known for their straightforward coupling to gold surface atoms. We used a two-step scheme involving chloromethylation of PS and then nucleophilic substitution of the chloromethyl groups with sodium hydrosulfide in ethanol (Scheme 1). We performed the first step in chloroform using a non-commercial chloromethylating agent prepared from butyl alcohol, paraformaldehyde and gaseous HCl at low temperature.[20] To verify successful completion of this stage, we performed a qualitative colorimetric test with nitrobenzyl pyridine (see ESI Fig. §2).[29] We then carried out the thiol-modification in ethanol, even though chloromethylated PS is probably only partially soluble in ethanol. We indirectly verified the success of this stage by mixing the resulting colloids with citrate-stabilized 12 nm gold particles. The excess of gold particles was removed by centrifugation. The resulting particles were redispersed in water and observed under TEM (Fig. 2). We used citrate-stabilized gold nanoparticles because citrate binds weakly to gold, and thus thiol groups readily displace citrate ligands. We found that the gold particles are attached only at the thiolated PS bumps within the dimples (Fig. 2). In control experiments (not shown) with chloromethylated PS bumps without thiol-modification, we saw no gold nanoparticle adsorption.

To take advantage of this specific adsorption site for gold nanoparticles within the dimples, we investigated methods for promoting and directing subsequent gold growth in order to obtain larger gold satellites within each dimple. The main challenges were (1) preserving the gold/thiol bonds, (2) restricting gold growth to the dimple area to preserve the tetrahedral symmetry of the nanostructure, and (3) ultimately obtaining gold/silica tetrapods (Scheme 1). The seeds act as efficient redox catalysts for metal ion reduction, which occurs selectively at their surface, as the energetic barrier for heterogeneous nucleation is much lower than that for homogeneous nucleation. In the literature, many seed-mediated recipes based on the use of citrate-capped gold seeds and chloroauric acid as a gold source have been reported. Three of them are particularly relevant here since they can yield gold particles with diameters of up to 200 nm.[30-32] We investigated each of them to assess their applicability for gold growth from the 12 nm gold seeds within our dimples. In all cases, for the sake of simplicity, we assumed one gold seed per dimple in our colloids, on average.

The first recipe uses ascorbic acid as a reducing agent and cetyltrimethylammonium bromide (CTAB) as a surfactant. This approach produces quasi-spherical gold particles up to 180 nm in diameter with a narrow size.[30] Unfortunately, in our experiments with citrate-capped gold particles anchored to the dimple surface, the procedure yielded quite complex and aggregated objects. Not only did most of the gold structures exhibit highly non-spherical shapes, but also they detached from the dimple areas (Fig. 3). We assume this failure is due to CTAB detrimentally affecting the gold-thiol bonding.

The second recipe, performed at 90°C in the presence of sodium citrate as a reducing and capping agent, generally yields uniform spherical gold particles with diameters of tens of nanometers.[31] We implemented this multi-step procedure for seeded growth on the surface of our particles' dimples. Starting from 12-nm particles and repeating the process up to 9 times, we found that this approach can produce gold

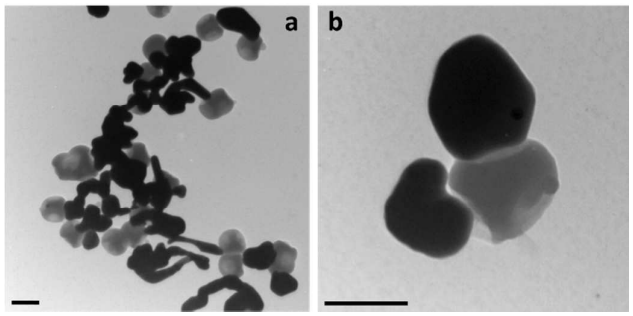

Figure 3: Transmission electron micrographs of gold/silica nanostructures obtained after gold regrowth performed in the presence of ascorbic acid and CTAB. Scale bars are 100 nm.

satellites with diameters of about 90 nm or even larger. In contrast, the previous recipe yields gold particles that remain attached to the dimples and that are relatively spherical (Fig. 4). However, the silica cores show damage from the successive treatments. After the ninth step, it becomes difficult to identify the core morphology. We assume the silica cores experience gradual etching due to the presence of sodium ions (counter-ions of the citrate precursor) in the reaction medium. This hypothesis is consistent with other experimental[33] and theoretical[34] studies in the literature. Moreover, the reduction process occurred at 90°C, which has been reported as harsh conditions for silica.[35]

The UV-visible spectra of these plasmonic nanoclusters agree with these overall observations. The surface plasmon resonance (SPR) band redshifts with increasing particle size. It peaks at 524 nm after one regrowth step, 531 nm after three, 538 nm after six, and 548 nm after nine. We also observe a large SPR broadening and increased scattering during the cyclic growth process. The gradual dissolution of the silica cores led to uncontrolled distances between the gold satellites. This in turn gives rise to uneven optical coupling between the gold particles, which broadens the absorption band

Overall, we found that this second recipe is sufficient for enlarging the gold seeds while preserving their positions within the dimples. However, the silica particles do not fare well through the many iterations necessary for obtaining large gold satellites.

The third recipe uses milder reduction conditions (ascorbic acid and sodium citrate at room temperature) and is reportedly capable of producing free gold particles with diameters in the range of 15-300 nm.[32] When we applied this recipe to our system, we found encouraging results as shown in the series of TEM images in Fig. 5. The reduction of the metallic precursor led to the gradual growth of the gold satellites onto the silica surface, and the dimpled silica particles were only slightly damaged. The gold nanoparticles remained strongly anchored to the dimples during the growth iterations and the largest satellites reached sizes of 120-140 nm after three cycles. We observe single gold satellites in a majority of the dimples, particularly on silica cores with a tetrahedral arrangement of dimples. The gold satellites are

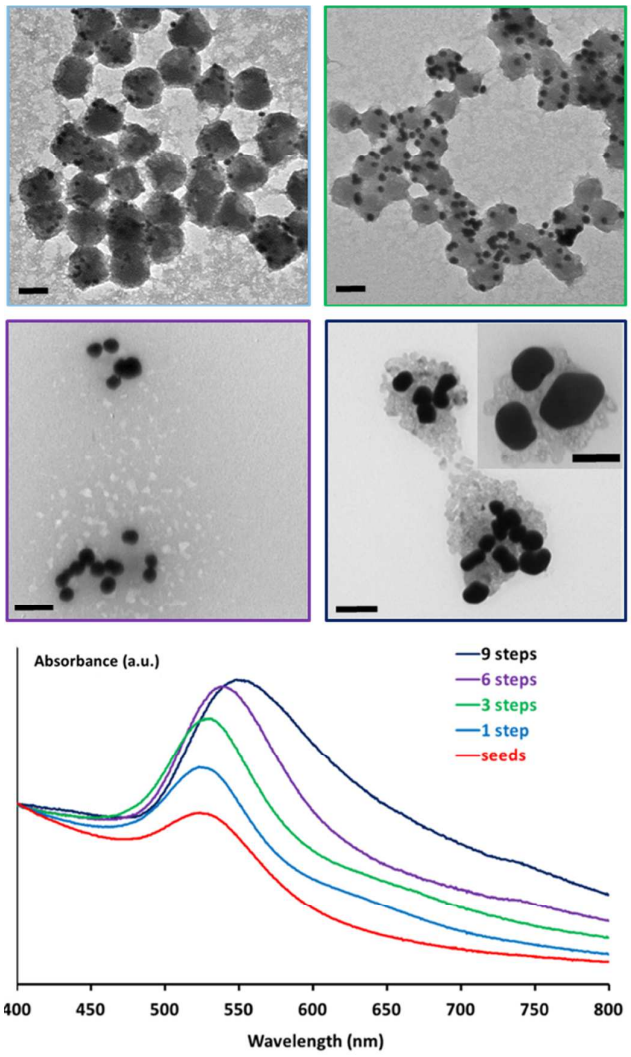

Figure 4: Transmission electron micrographs and corresponding UV-visible spectra (normalized at 400 nm) of gold/silica nanostructures obtained after 1, 3, 6, and 9 growth iterations performed in the presence of sodium citrate at 90°C. Scale bars are 100 nm.

more oblate than spherical. These silica/gold nanostructures are stable for more than one month, but they sediment quickly due to their high mass.

We measured the optical properties of these core/satellites clusters during the growth process, as shown in Fig. 5. As expected, the electric dipole surface plasmon resonance redshifted with increasing gold satellite size. We found increased scattering with successive growth iterations as well.

4 Conclusion

We have shown that the PS macromolecules are grafted at the bottom of the dimples in our silica particles due to the copolymerization of styrene and MMS-derived grafts. These macromolecules are long and easily thiol-modified, which

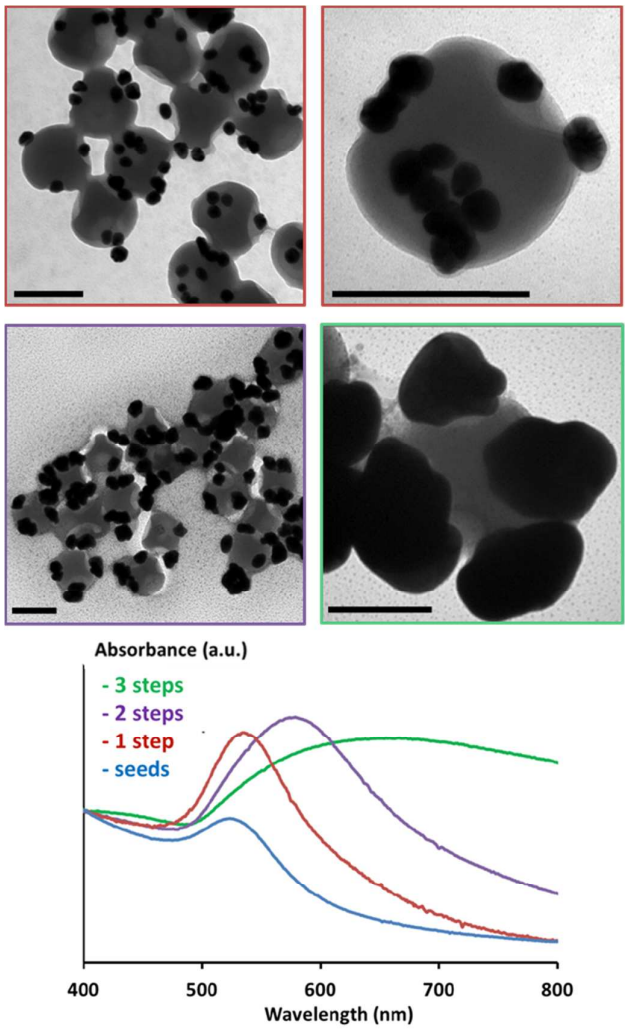

Figure 5: Transmission electron micrographs and corresponding UV-visible spectra (normalized at 400 nm) of gold/silica nanoclusters obtained after 1, 2, or 3 growth iterations performed in the presence of sodium citrate and ascorbic acid at room temperature. Scale bars are 100 nm.

makes them suitable adsorption sites for citrate-stabilized gold nanoparticles. Our efforts to grow larger gold satellites, using the adsorbed nanoparticles as seeds, led to moderate success. Two key factors arise for minimizing polydispersity and controlling the gold satellite morphologies and positions: (1) the applied mixture of ascorbic acid and sodium citrate as reducing and stabilizing agents, and (2) the process of slowly adding separate reducing and precursor solutions at room temperature, as demonstrated in the third recipe. These mild reaction conditions preserve the gold satellite positions within the dimples as well as the geometry of the dimpled silica cores. This procedure yields well-defined gold patches with diameters up to 140 nm, although they are not perfectly spherical. The tetrahedral symmetry of the dimpled structure is preserved throughout the growth of the gold satellites.

The surface functionality of these structures means that they have potential for further chemical modification and may find use in colloidal self-assembly schemes. Moreover, these gold clusters could be useful in their own right as elements of optical metafluids due to their tetrahedral symmetry and plasmonic properties.[36]

Acknowledgements

TEM experiments were performed at the Plateforme de Caractérisation des Matériaux and Bordeaux Imaging Center of the University of Bordeaux. This work was supported by the LabEx AMADEus (ANR-10-LABX-42) and IdEx Bordeaux (ANR-10-IDEX-03-02), *i.e.* the Investissements d'Avenir programme of the French government managed by the Agence Nationale de la Recherche.

References

1 A. Van Blaaderen, *Nature*, 2006, **439**, 545.
2 F. Li, D. P. Josephson and A. Stein, *Angew. Chem. Int. Ed.*, 2011, **50**, 360.
3 S. Sacanna, D. J. Pine and G.-R. Yi, *Soft Matter*, 2013, **9**, 8096.
4 E. Duguet, C. Hubert, C. Chomette, A. Perro and S. Ravaine, *C. R. Chim.*, DOI:10.1016/j.crci.2015.11.013.
5 Q. Chen, S. C. Bae and S. Granick, *Nature*, 2011, **469**, 381.
6 S. Sacanna, W.T.M. Irvine, P.M. Chaikin and D. J. Pine, *Nature* 2010, **464**, 575.
7 Y. Wang, Y. Wang, D. R. Breed, V. N. Manoharan, L. Fen, A. D. Hollingsworth, M. Weck and D. J. Pine, *Nature*, 2012, **491**, 51.
8 G. Zhang, D. Wang and H. Möhwald, *Nano Lett.*, 2005, **5**, 143.
9 A. B. Pawar and I. Kretzschmar, *Langmuir*, 2008, **24**, 355; A. B. Pawar and I. Kretzschmar, *Langmuir*, 2009, **25**, 9057.
10 H. Bao, B. Butz, Z. Zhou, E. Spiecker, M. Hartmann and R. N. Klupp Taylor, *Langmuir*, 2012, **28**, 8971.
11 R. N. Klupp Taylor, H. X. Bao, C. T. Tian, S. Vasylyev and W. Peukert, *Langmuir*, 2010, **26**, 13564.
12 S.J. Oldenburg, R.D. Averitt, S.L. Westcott and N.J. Halas, *Chem. Phys. Lett.*, 1998, **288**, 243.
13 J. Yang, Y. Li, L. Zu, L. Tong, G. Liu, Y. Qin and D. Shi, *ACS Appl. Mater. Interfaces*, 2015, **7**, 8200.
14 H. Bao, T. Bihr, A.-S. Smith and R. N. Klupp Taylor, *Nanoscale*, 2014, **6**, 3954.
15 S. H. Kim, G. R. Yi, K. H. Kim and S. M. Yang, *Langmuir*, 2008, **24**, 2365.
16 D. J. Kraft, J. Hilhorst, M. A. P. Heinen, M. J. Hoogenraad, B. Luigjes and W. K. Kegel, *J. Phys. Chem. B*, 2011, **115**, 7175.
17 Y. Wang, Y. Wang, X. Zheng, G. R. Yi, S. Sacanna, D. J. Pine and M. Weck, *J. Am. Chem. Soc.*, 2014, **136**, 6866.
18 A. Désert, C. Hubert, Z. Fu; L. Moulet, J. Majimel, P. Barboteau, A. Thill, M. Lansalot, E. Bourgeat-Lami, E. Duguet and S. Ravaine, *Angew. Chem. Int. Ed.*, 2013, **52**, 11068.
19 C. Hubert, C. Chomette, A. Désert, M. Sun, M. Treguer-Delapierre, S. Mornet, A. Perro, E. Duguet and S. Ravaine, *Faraday Discuss.*, 2015, **181**, 139.
20 A. Warshawsky and A. Deshe, *J. Polym. Sci., Polym. Chem.*, 1985, **23**, 1839.
21 A. Perro, E. Duguet, O. Lambert, J.-C. Taveau, E. Bourgeat-Lami and S. Ravaine, *Angew. Chem., Int. Ed.*, 2009, **121**, 367.
22 A. Désert, I. Chaduc, S. Fouilloux, J.-C. Taveau, O. Lambert, M. Lansalot, E. Bourgeat-Lami, A. Thill, O. Spalla, S. Ravaine and E. Duguet, *Polym. Chem.*, 2012, **3**, 1130.
23 A. Désert, J. Morele, J. C. Taveau, O. Lambert, M. Lansalot, E. Bourgeat-Lami, A. Thill, O. Spalla, L. Belloni, S. Ravaine and E. Duguet, *Nanoscale*, DOI: 10.1039/C5NR07613G.
24 A. Wang, H. P. Ng, Y. Xu, Y. Li, Y. Zheng, J. Yu, F. Han, F. Peng and L. Fu, *J. Nanomater.*, 2014, **2014**, 1.

25 A. Perro, D. Nguyen, S. Ravaine, E. Bourgeat-Lami, O. Lambert, J. C. Taveau and E. Duguet, *J. Mater. Chem.*, 2009, **19**, 4225.
26 D. Yin, Q. Zhang, H. Zhang and C. Yin, *J. Polym. Res.*, 2009, **17**, 689.
27 A. Guyot and P. Espiard, *Polymer*, 1995, **36**, 4391.
28 Z. Zeng, J. Yu and Z.-X. Guo, *Macromol. Chem. Phys.*, 2005, **206**, 1558.
29 F. Galindo, B. Altava, M. I. Burguete, R. Gavara and S. V Luis, *J. Comb. Chem.*, 2004, **6**, 859.
30 J. Rodríguez-Fernández, J. Pérez-Juste, F. J. García De Abajo and L. M. Liz-Marzán, *Langmuir*, 2006, **22**, 7007.
31 N. G. Bastus, J. Comenge and V. Puntes, *Langmuir*, 2011, **27**, 11098.
32 C. Ziegler and A. Eychmüller, *J. Phys. Chem. C*, 2011, **115**, 4502.
33 E. Mahon, D. R. Hristov and K. A Dawson, *Chem. Commun.*, 2012, **48**, 7970.
34 P. M. Dove, N. Han, A. F. Wallace and J. J. De Yoreo, *Proc. Natl. Acad. Sci. U. S. A.*, 2008, **105**, 9903.
35 Y. J. Wong, L. Zhu, W. S. Teo, Y. W. Tan, Y. Yang, C. Wang and H. Chen, *J. Am. Chem. Soc.*, 2011, **133**, 11422.
36 Y. A. Urzhumov, G. Shvets, J. Fan, F. Capasso, D. Brandl and P. Nordlander, *Opt. Express*, 2007, **15**, 14129.